

## Evaluating the use of weathering indices for determining mean annual precipitation in the ancient stratigraphic record

Jason S. Adams<sup>a</sup>, Mary J. Kraus<sup>a,\*</sup>, Scott L. Wing<sup>b</sup>

<sup>a</sup> Department of Geological Sciences, University of Colorado, Boulder, CO 80309-0399, USA

<sup>b</sup> Department of Paleobiology, Smithsonian Museum of Natural History, Washington, DC 20560, USA

### ARTICLE INFO

#### Article history:

Received 21 April 2011

Received in revised form 1 July 2011

Accepted 3 July 2011

Available online 8 July 2011

#### Keywords:

Paleosol

Weathering index

Paleoclimate

Vertisol

Paleocene–Eocene Thermal Maximum

Global warming

### ABSTRACT

Different quantitative methods have been developed to determine paleo-rainfall using paleosols. Of particular interest are methods that use bulk geochemistry to calculate a weathering index and, from that, mean annual precipitation. Twenty-three paleosols that formed during a time of significant climate change—the Paleocene–Eocene Thermal Maximum (PETM)—were analyzed to evaluate the relative merits of two geochemical proxies that have been developed for estimating paleoprecipitation: one depends on the chemical index of alteration without potash (CIA-K) and the other uses the CALMAG weathering index, which depends on CaO and MgO. The paleosols are located in the Paleogene Fort Union and Willwood formations in the Bighorn Basin, WY. Morphologic differences among the paleosols indicate that they formed under varied soil moisture conditions. A morphology index was developed from pedogenic features that are sensitive to soil drainage, and thus to rainfall, to assess that variability. Quantitative mean annual precipitation (MAP) values were calculated for each paleosol using the CIA-K index and the CALMAG index, which was developed specifically for Vertisols. Those results were compared to the morphology index for 23 paleosols.

The results indicate that increases and decreases in MAP calculated from both methods correlate relatively well to changes in the soil morphology index; however, the results from the CALMAG weathering index show a stronger correlation. The results suggest that the CALMAG proxy provides a more robust MAP estimate for Vertisols. In addition to comparing MAP estimates to the soil morphology index, we compared the MAP values to paleorainfall estimates determined from paleofloras at the same stratigraphic levels as three of the paleosols. That comparison confirms that the CALMAG method is reliable for reconstructing MAP from ancient Vertisols. The results also show that, in the Bighorn Basin, Vertisols with a B horizon <1 m thick should not be used to determine MAP. Thinner paleosols have had less time for weathering and may not have cation distributions representative of precipitation.

© 2011 Elsevier B.V. All rights reserved.

### 1. Introduction

With increased interest in reconstructing paleoclimates, various quantitative approaches have been developed for estimating mean annual precipitation (MAP). Methods for quantitatively determining MAP include plant fossils and paleosol attributes, especially geochemical properties. Fossil leaves and palynomorphs are of value because relationships exist between modern plant physiognomy and MAP (e.g., Wolfe, 1995; Wiemann et al., 1998; Wilf et al., 1998; Jacobs, 1999; Wolfe and Spicer, 1999; Gregory-Wodzicki, 2000; Jacobs and Herendeen, 2004; Peppe et al., 2011), and also because the nearest living relatives of fossil plants often have similar climatic tolerances (e.g., Greenwood and Wing, 1995). Vertebrate fossils, representing

community assemblages, can also be used to determine MAP, but they have not been used on strata older than Miocene time (e.g., Böhme et al., 2006; van Dam, 2006). Paleosols are an important source of paleoclimate data because they are vertically stacked, and thus provide a continuous and highly resolved temporal record of paleoclimate. In addition, paleosols are common throughout the continental stratigraphic record, both temporally and geographically. Paleosol-based methods for estimating MAP include geochemical analysis of iron–manganese (Fe–Mn) nodules (Stiles et al., 2001) and depth to horizons enriched in pedogenic carbonate (e.g., Retallack, 1994). Not all paleosols contain either Fe nodules or carbonate, thus, there has been considerable interest in a MAP proxy developed by Sheldon et al. (2002), based on a chemical index of weathering or alteration (CIA) that excludes potassium (CIA-K).

The Sheldon et al. (2002) method is attractive because it is determined from readily available bulk geochemical data; however, restrictions on its use are recognized. This method can only be used on paleosols containing less than 5% bulk carbonate and no carbonate

\* Corresponding author at: Department of Geological Sciences, UCB 399, 2200 Colorado Ave., University of Colorado, Boulder, CO 80309-0399, USA. Tel.: +1 303 492 7251; fax: +1 303 492 2606.

E-mail address: [mary.kraus@colorado.edu](mailto:mary.kraus@colorado.edu) (M.J. Kraus).

nodules (e.g., Prochnow et al., 2006), and it is not appropriate for waterlogged (gley) soils or soils that lack a marked difference in weathering index between the B horizon and parent material (Sheldon et al., 2002; Sheldon and Tabor, 2009). Other difficulties and uncertainties arise when attempting to use the CIA-K technique. Although Sheldon et al. (2002) and Sheldon and Tabor (2009) indicated that the Bw or Bt horizon should be sampled, the B horizons of many paleosols can be subdivided (e.g., B<sub>1</sub>, B<sub>2</sub> horizons) based on different morphologic attributes, and the different parts reflect complicated depositional and/or pedogenic histories. To address these uncertainties for multipart B horizons, Prochnow et al. (2006) sampled the first subsurface argillic or cambic horizon of a mature paleosol profile, and Kraus and Riggins (2007) used the most strongly weathered subunit of a B horizon to determine MAP.

The Sheldon et al. (2002) method is a seminal approach to using paleosols for paleoclimatic reconstruction, and it has been widely used to interpret paleoprecipitation from paleosols through much of Phanerozoic time (e.g., Driese et al., 2005; Prochnow et al., 2006; Kraus and Riggins, 2007). Many of the paleosols that have been studied are Vertisols, which are widespread in fluvial strata. Nordt and Driese (2010) concluded that Vertisols deserve their own quantitative approach to MAP because their parent material—“inherited clay”—has a significant impact on the abundances and distribution of bulk soil oxides. Consequently, Vertisols differ from the wide variety of soils on which the Sheldon climofunction was developed. Nordt and Driese (2010) proposed a modified weathering index—the CALMAG index—to determine MAP specifically for Vertisols. However, development and evaluation of CALMAG has focused primarily on modern Vertisols, and includes very limited testing in the paleosol record.

The main goal of the current study is to evaluate the relative merits of the CIA-K and CALMAG approaches to estimating MAP for Vertisols through analysis of 23 paleosols in Paleogene strata from the Bighorn Basin, Wyoming. The paleosols, all of which are Vertisols, are excellent for testing quantitative approaches to MAP because they formed during a time of documented climate change—the Paleocene–Eocene Thermal Maximum. Previous studies of coeval paleosols in two other areas of the Bighorn Basin show precipitation fluctuations during this time (Kraus and Riggins, 2007; Smith et al., 2008). Although the paleosols in this study formed during the PETM, this paper does not assess temporal changes in paleoprecipitation relative to the PETM, but focuses on the methods of MAP reconstruction.

First, this study describes the general morphology of the paleosols and introduces a soil morphology index that is based on soil properties that depend on soil moisture conditions. This index provides a simple, qualitative assessment of the moisture regime for each of the paleosols. Second, CIA-K and CALMAG were calculated for each of the paleosols. The quantitative precipitation results are compared to the morphology index to determine how reliable either approach is for ancient Vertisols. Finally, the quantitative MAP results are judged against paleobotanical estimates for MAP. The study also assesses the consistency of weathering indices through the B horizons of paleosols and how samples should be collected for both geochemical proxies.

## 2. Weathering indices and paleoprecipitation

The Sheldon et al. (2002) method, based on a soil weathering index developed by Harnois (1988) and Maynard (1992), compares abundances of soluble cations—calcium (Ca) and sodium (Na)—against relatively stable aluminum (Al) to determine the relative amount of chemical weathering. Because diagenesis can yield elevated potassium (K) concentrations in paleosols, this chemical index omits K and is termed CIA-K. The intensity of weathering depends, in part, on precipitation, and Sheldon et al. (2002) developed an empirical relationship relating MAP to CIA-K using soil molecular oxide data from Marbut (1935).

The Sheldon et al. (2002) equations for CIA-K and MAP are shown below. The published error associated with the regression analysis is  $\pm 181$  mm (Sheldon et al., 2002; Sheldon and Tabor, 2009).

$$\text{CIA-K} = [\text{Al}_2\text{O}_3 / (\text{Al}_2\text{O}_3 + \text{CaO} + \text{Na}_2\text{O})] \times 100 \quad (1)$$

$$\text{MAP (millimeters/year)} = 221e^{0.0197 * \text{CIA-K}}; r^2 = 0.72 \quad (2)$$

Driese et al. (2005) found that Eq. (2) underestimates MAP for modern Vertisols in Texas. In a subsequent study, Nordt and Driese (2010) concluded that the most reliable MAP estimates for Vertisols are derived from an index that substitutes MgO for Na<sub>2</sub>O. They proposed the CALMAG index, which is an analog to the CIA-K index but based on CaO and MgO. Nordt and Driese also developed an empirical equation relating MAP to CALMAG:

$$\text{CALMAG} = [\text{Al}_2\text{O}_3 / (\text{Al}_2\text{O}_3 + \text{CaO} + \text{MgO})] \times 100 \quad (3)$$

$$\text{MAP} = 22.69 * \text{CALMAG} - 435.8 \quad r^2 = 0.90 \quad (4)$$

The standard error for this relationship is  $\pm 108$  mm. Nordt and Driese found that oxide values varied little within the 25 to 100 cm depth interval of individual profiles, and they used a weighted average of the base oxides to calculate MAP for a particular soil. Their sampling of the B horizons focused on sampling each subdivision of that B horizon.

## 3. Geological background

Paleosols that formed in the Bighorn Basin, Wyoming developed on fine-grained alluvial deposits in the uppermost Fort Union and lowermost Willwood formations. This study focuses on paleosols in the southeastern Bighorn Basin (Fig. 1). Evidence for the carbon isotope excursion (CIE) that is used to recognize the PETM interval comes from bulk organic matter and n-alkanes from paleosols (Wing et al., 2005; Smith et al., 2007). Those studies place the Paleocene–Eocene boundary at the base of the Willwood Formation in the study areas. Both isotopic analyses of fossil material (Fricke et al., 1998;

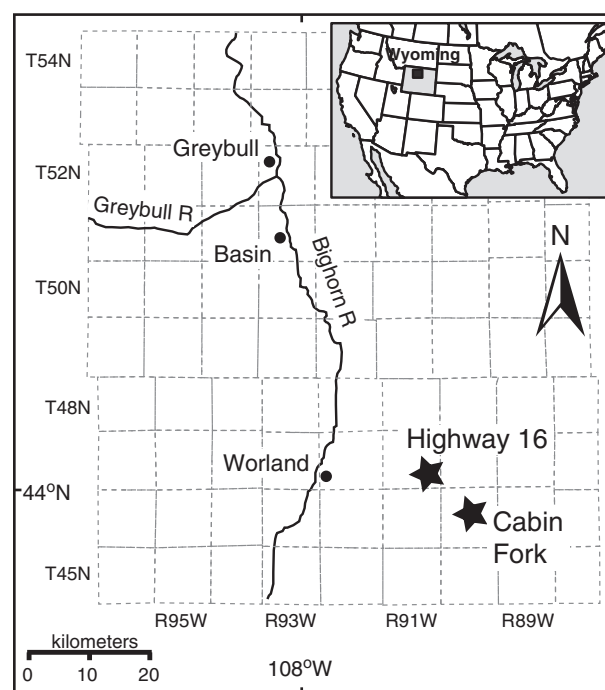


Fig. 1. Map showing the eastern Bighorn Basin and study areas at Highway 16 and Cabin Fork. Inset map shows location of Bighorn Basin in northern Wyoming, U.S.A.

Fricke and Wing, 2004) and leaf margin analysis (Wing et al., 2005) of terrestrial megafloras indicate that temperatures in the Bighorn Basin rose  $\sim 5$  °C during the PETM. The isotopes suggest that mean annual temperature (MAT) reached 26 °C, and the leaf analysis produces an estimate of MAT of  $\sim 20$  °C, (Wing et al., 2005). Wing et al. suggested that the plants probably underestimate MAT because many of those studied are riparian and wetland plants.

#### 4. Methods

The study includes data from 23 paleosols from two study areas in the southeastern Bighorn Basin: Highway 16 (HW16) and Cabin Fork (CF) (Fig. 1). To assess the importance of time on weathering indices, paleosol profiles of various thickness were studied. Ten of the paleosols have B horizons <1 m thick and 13 have B horizons >1 m thick (Table 1).

Sections were measured by digging  $\sim 1$  meter wide trenches down to fresh rock. Paleosol field units were designated on the basis of grain size, matrix and mottle colors, abundance and type of nodules, shrink-swell features, and rhizolith preservation. Hand sample and field descriptions are based on methods detailed in the *Soil Survey Manual* (Soil Survey Division Staff, 1993).

Samples were analyzed for major element oxides using a KeveX 0700 X-ray fluorescence spectrometer at the University of Colorado Laboratory for Environmental and Geological Studies (LEGS). Weight percents given by XRF were recalculated to molar ratios, following Sheldon et al. (2002), for use in chemical weathering analyses. Quantitative grain sizes were determined using a Malvern Longbed Mastersizer.

Three of the paleosols contain carbonate nodules (Table 1). These were analyzed, despite caveats concerning application of the Sheldon et al. (2002) method, because in all three cases the weight percent carbonate in the matrix was less than 2%. Paleosols with carbonate nodules and bulk carbonate greater than 2% were eliminated from consideration.

#### 5. Paleosol morphology and soil moisture

Like the Vertisols on which the CAL-MAG approach was developed, the Willwood paleosols formed on floodplain alluvium with relatively high clay content. Quantitative grain size analyses of random samples of the paleosols show that clay content is generally >40% and a number of samples have >60% clay content (Appendix B). Clays throughout the Willwood Formation are dominated by mixed layer illite/smectite (e.g., Gibson et al., 2000; Kraus and Riggins, 2007).

The paleosols in the study area are similar to Willwood paleosols described from PETM strata in other parts of the Bighorn Basin (Kraus and Hasiotis, 2006; Kraus and Riggins, 2007). All paleosols described in this study are interpreted as vertic paleosols based on the relatively high clay content, most of which is smectitic; presence of abundant, commonly intersecting, slickensides; and recognition of muklara structures (Fig. 2) (Soil Survey Staff, 1993). Evaluated paleosols range from moderately well-drained with red B horizons to more poorly-drained paleosols with purple B horizons. Both red matrix and purple matrix have similar hues, commonly 2.5R, 5R, and 10R. However, soil matrix that is purple consistently has chromas of 1 or 2, which is consistent with more poorly drained conditions (e.g., Vepraskas, 2001). In contrast, red colors have chromas of 4 or higher.

The CIA-K proxy for precipitation is more robust if samples are taken from Vertisol microlows (Driese et al., 2005). Recognizing such microtopography in paleosols from our field area is complicated, however. Topographic lows are readily identified by lenticular or bowl-shaped, gley-dominated peds bounded by slickensides (e.g., Lynn and Williams, 1992; Driese et al., 2005), but long-term floodplain aggradation and shifts in floodplain topography can obscure expression of these features in a vertical profile. Soil features that probably developed in older microlows can be subsequently located directly below microhighs and *vice versa*, thus complicating interpretations of microtopographic influence through a mature vertical profile. The paleotopographic setting of any vertical section can only be confirmed by lateral investigation of the paleosol profile.

**Table 1**  
Calculated morphology indices, calculated MAP values, and B horizon thicknesses for paleosols in the study areas. Mean MAP values are the average of MAP values calculated for the upper 50 cm of each paleosol B horizon; Maximum values are the highest MAP value from the upper 50 cm of each B horizon. \*\* indicates paleosols containing carbonate nodules; \*\*1 indicates paleosol for which CIA-MAP Max was determined from a lower B horizon with no carbonate.

Trench and unit	Morphology index	CAL-MAP		CIA-MAP		B horizon thickness (m)
		Mean (mm)	Max (mm)	Mean (mm)	Max (mm)	
HW16-08-02	8.6	1115	1172	1131	1251	0.5
HW16-08-04 (unit 1)	8.0	1198	1237	1221	1270	0.5
HW16-08-4 (unit 4)	11.0	1190	1206	1215	1236	0.5
CUCF-07-05-10	7.0	1219	1243	1239	1256	0.5
CUCF-07-01	9.1	1266	1297	1252	1269	0.5
HW16-08-01 (unit14)**1	15.8	1106	1150	1178	1212	0.6
CUCF-07-07-2	7.0	1213	1224	1245	1269	0.6
HW16-08-19 (unit 13)**	13.0	967	967	999	999	0.6
HW16-08-15	8.3	1123	1206	1159	1290	0.8
HW16-08-20 (unit 8)	8.0	1250	1267	1267	1296	0.8
CUCF-07-04-2**	13.7	1099	1175	1112	1209	1.0
HW16-08-1 (unit 20)	10.8	1162	1175	1182	1215	1.0
HW16-08-05	5.7	1214	1220	1264	1275	1.1
HW16-08-17	8.3	1162	1197	1279	1309	1.1
HW16-08-19 (unit 2)	12.0	1172	1191	1211	1223	1.1
CUCF-07-05-4	2.2	1248	1272	1211	1244	1.1
HW16-08-20 (unit 5)	8.0	1240	1284	1200	1271	1.2
HW16-08-14	6.4	1254	1284	1346	1367	1.4
HW16-08-07	4.3	1189	1219	1160	1234	1.5
HW16-08-06	2.0	1271	1282	1278	1284	1.6
CUCF-07-02-1	3.5	1233	1248	1233	1253	1.6
CUCF-07-02-7	4.6	1269	1277	1251	1272	1.7
HW16-08-08	3.5	1240	1255	1251	1281	1.9

**Table 2**

Points assigned for soil carbonate and yellow-brown nodules in determining the morphology index for each paleosol.

	Wetter soil conditions	Intermediate conditions	Drier soil conditions
Features	0 points	3 points	6 points
Soil carbonate	no carbonate	Calcareous rhizoliths small (<mm) nodules	Larger (>mm) nodules
Yellow-brown nodules	Common to abundant	Sparse	Absent

### 5.1. Paleosol morphology index

Three morphologic features with soil wetness significance—matrix chroma, pedogenic carbonate, and yellow-brown nodules—were combined to develop a simple index of soil moisture. Although this index provides only a relative assessment of soil drainage, it can be used to assess changes in drainage through a vertical section of paleosols. The index can also be used as a morphologic test of the geochemical MAP results.

Following the approach used in chronosequence studies (e.g., Harden, 1982; Vidic and Lobnik, 1997; Calero et al., 2008), a numerical value was assigned to each property for either the entire B horizon, if thin, or for subdivisions of thicker B horizons that could be subdivided on morphologic grounds. Most B horizons can be subdivided, and, in those cases, the property value for each subdivision was multiplied by subdivision thickness. The points were summed for all subdivisions of each paleosol, and the sum divided by total thickness of the B horizon to yield a morphology index for the profile (Appendix A).

Studies have shown that matrix chroma decreases as the length of soil saturation increases, and low chroma ( $\leq 2$ ) matrix colors are commonly linked to seasonal saturation and gleying of soils (e.g., Evans and Franzmeier, 1986; Veneman et al., 1998). The degree to which paleosol colors reflect pedogenesis versus burial diagenesis has been debated (e.g., Retallack, 1991; Blodgett et al., 1993; PiPujol and Buurman, 1994). The co-existence of red and yellow-brown colors, as seen in the Willwood paleosols, was considered evidence for pedogenesis rather than diagenetic recoloration by PiPujol and Buurman (1994), who also noted that such color patterns resemble those of modern soils and, if diagenesis were responsible, all iron compounds should have been changed in a similar way. It has also



**Fig. 2.** Photograph of preserved mukkkara structures and associated morphologic contrasts between microhighs and microlows in a paleo-Vertisol from Cabin Fork. Microlows at the top of the profile are bounded by large slickensides and are characterized by low chroma colors. Dashed line marks base of bowl-shaped morphology. Heavy black line marks top of a rooted horizon. Thinner black lines delineate low-chroma lenses interpreted to have formed in previous microlows that were subsequently buried. Previous microlows now exist under preserved microhighs. Hat is 40 cm long.

been argued that, even if original colors are not preserved exactly, the colors seen today are useful because they represent environmentally-controlled differences in iron-bearing minerals at the time of formation (Wells et al., 2002; Demko et al., 2004). Chroma has been used in other paleosol studies to support poorly drained versus well drained and oxygenated conditions (e.g., Wells et al., 2002; Driese and Ober, 2005). Thus, chroma is viewed as a useful approach to interpreting past soil drainage conditions. Matrix chromas were determined using Munsell color charts on dry samples. Values ranged from 2 (wetter paleosols) to 6 (drier paleosols).

Calcium carbonate nodules are common in many parts of the Willwood Formation, and they are abundant in PETM outcrops at Polecat Bench (e.g., Kraus and Riggins, 2007). In the study area, calcium carbonate is present as nodules or calcareous rhizoliths only in paleosols within the main body of the CIE. In fact, the onset of the CIE corresponds to the stratigraphically lowest carbonate nodules, and the top of the “body” of the CIE (sensu Bowen et al., 2006) corresponds to the highest carbonate as nodules or rhizoliths. Although the relationship between pedogenic carbonate and MAP is complicated (e.g., Blodgett, 1988), the presence or absence of carbonate nodules can be used to separate lower MAP from higher MAP areas (e.g., Nordt et al., 2006). More specifically, nodules are more common in soils that form in seasonal climates with MAP estimated as <760 mm (Royer, 1999) to <1000 mm (Retallack, 1994). The development of calcite associated with roots and root channels is common in some Willwood paleosols (Kraus and Hasiotis, 2006). Similarly, calcitic rhizoliths are common in regions where evapotranspiration is greater than effective precipitation (e.g., Brady and Weil, 1999), and various authors (e.g., Becze-Deak et al., 1997; PiPujol and Buurman, 1997) attribute the formation of calcite in root channels to seasonal climates during a pronounced dry season. Episodic rains introduce water into the soil channels, and, if the water contains easily solubilized calcium carbonate, micrite precipitates when the soil dries. Kraus and Hasiotis (2006) found calcitic rhizoliths characteristic of paleosols that were at least moderately drained.

Because chroma ranged from 2 to 6 for paleosols in the study area, 6 points was the maximum value assigned to each of the other characters. Thus, for carbonate, the absence of both carbonate nodules and calcite rhizoliths (wetter soils) in each B horizon or subdivision of the B horizon is scored as 0 points, 3 points are assigned if calcareous rhizoliths or only sparse, small nodules (somewhat drier) are present, and the presence of carbonate nodules (drier) is scored as 6 points (Table 2).

Yellow-brown nodules in the study area are dominated by iron (Fe ranges from 7.8 to ~30 wt.%) and contain only small amounts of manganese (0.03 to 0.16 wt.%). Similar Fe or Fe–Mn nodules grow during wet/dry cycles in response to changing redox conditions (e.g., White and Dixon, 1996; Stiles et al., 2001) and are more characteristic of soils that undergo seasonal waterlogging (e.g., Ransom et al., 1987; McKenzie, 1989). Schwertmann and Fanning (1976) found that such nodules increase in abundance and size as soil wetness increases; however they are absent from very poorly drained soils. Stiles et al. (2001) pointed out that, if the texture and landscape position of various soils are similar, precipitation has a significant influence on the formation of ferruginous nodules. A unit with common to abundant ferruginous nodules (wetter soils) is scored as 0 points, 3 points are assigned to units with sparse nodules, and the absence of yellow-brown nodules is scored as 6 points (Table 2). Yellow-brown and carbonate nodules have inverse scoring schemes because carbonate nodules indicate drier conditions (high points) whereas yellow-brown nodules indicate wetter soil conditions (low points).

The least well drained soils have morphology indices of approximately 2, and the best-drained paleosols approach an index of 18, which is the maximum value possible. Examples are shown in Fig. 3, and indices for all paleosols are provided in Appendix A. Paleosol A has an index of 13.7 because it has a relatively high chroma of 6, carbonate nodules are present throughout, and yellow-brown nodules are absent

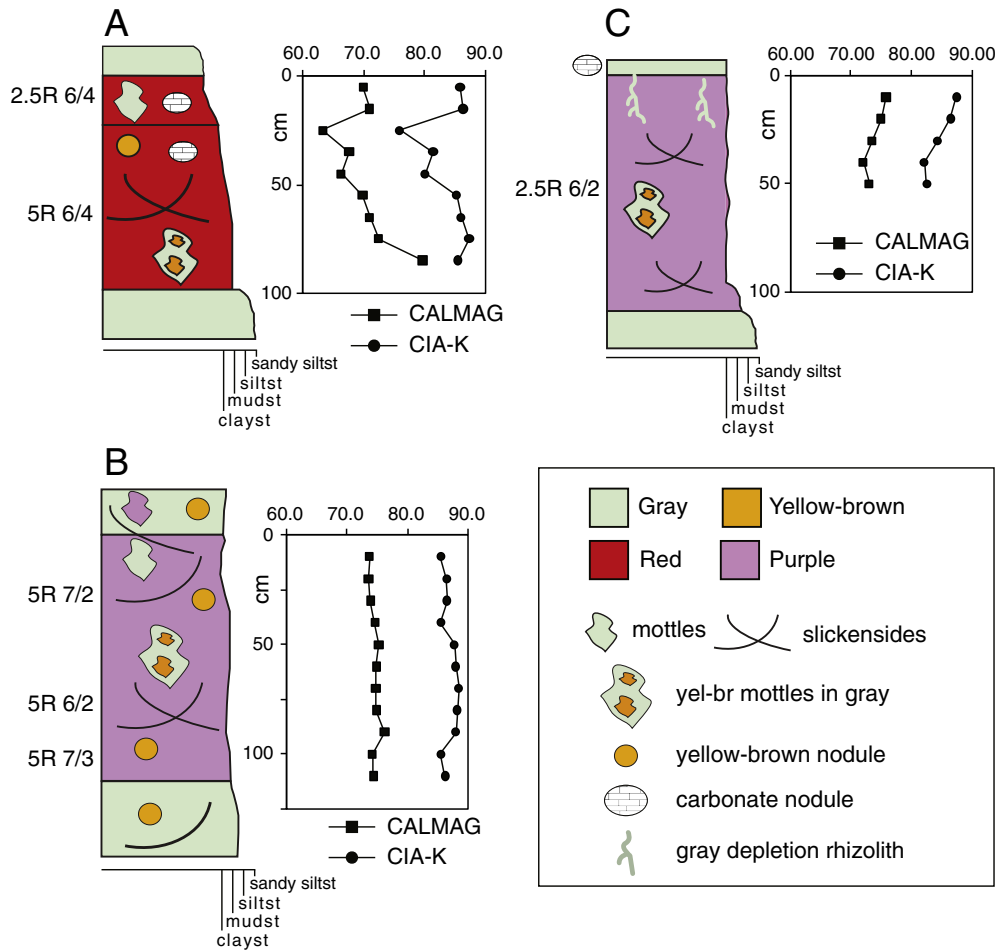


**Fig. 3.** Measured stratigraphic sections through three representative paleosols and CIA-K and CALMAG results plotted against depth for those profiles. A. Red paleosol (CUCF-07-04) from Cabin Fork. B. Purple paleosol (CUCF-07-05-4) from Cabin Fork. C. Purple paleosol (HW16-08-20) from Highway 16. Geochemical results for the profiles presented in Appendix B; morphology index results presented in Appendix A.

in the upper part of the B horizon, and, although present in the lower part of the B horizon, are only sparse. Paleosol B is at the opposite end of the spectrum with an index of only 2.2, which indicates poor drainage. Most of the B horizon has a chroma of only 2 and no carbonate is present. Furthermore, ferruginous nodules are abundant throughout. The morphology index for Paleosol C, which is 8.0, lies between those of paleosols A and B. This paleosol resembles paleosol B in that the B horizon has a chroma of only 2 and carbonate is absent (although present in the gray bed above). It shows drier soil conditions than B because ferruginous nodules are absent throughout.

The morphology index provides a quantitative means of assessing the relative soil moisture for a suite of paleosols; however, it does not provide a quantitative estimate of MAP the way the weathering indices do. Nonetheless, because MAP should rise when the morphology index decreases and *vice versa*, it presents one approach to assessing the CALMAG and CIA-K methods for estimating MAP for Vertisols. As the morphology index increases or decreases through a section of paleosols so too should the associated MAP value estimated by other methods.

## 6. Weathering indices and paleoprecipitation

Paleosol B horizons were sampled at 10 cm vertical intervals for geochemical analysis. This sampling interval is typical for detailed studies of elemental redistribution in soils (e.g., Driese, 2004). Four

thick (>1 m thick) paleosols were sampled to the bases of their B horizons; 4 were sampled to a depth of at least 90 cm and 5 to a depth of at least 60 cm. Depending on their total thickness, 1 to 6 samples were collected from B horizons of thinner paleosols (<1 m thick). CALMAG and CIA-K were calculated for each of these samples and the results are provided in Appendix B. Vertical trends in CALMAG and CIA-K were plotted for each paleosol. Visual examination of the plots confirms Nordt and Driese's (2010) finding that CALMAG values (and, thus, CALMAG-MAP estimates) vary little down profile in Vertisols (Fig. 3B and C). In addition, calculated standard deviations indicate tight clustering of CALMAG values around the mean for most B horizons (Appendix B). Similarly, CIA-K values show only modest down-profile variations (Fig. 3B and C).

Following Sheldon et al. (2002) and Nordt and Driese (2010), MAP values were determined from CIA-K and from CALMAG (Appendix B). The two MAP estimates are referred to as CIA-MAP and CAL-MAP. Because most paleosols have weathering index and MAP estimates at multiple stratigraphic levels in the B horizon, a method was needed to produce a summary MAP value for each paleosol. First, because we had multiple samples from the upper 50 cm of the B horizons of all paleosols examined, a mean MAP value was calculated for that upper 50 cm. Second, the maximum MAP value was determined for the upper 50 cm of each B horizon. Maximum and mean CAL-MAP and CIA-MAP values were plotted against the morphology index and regression analyses were completed (Figs. 4 and 5; Appendix B).

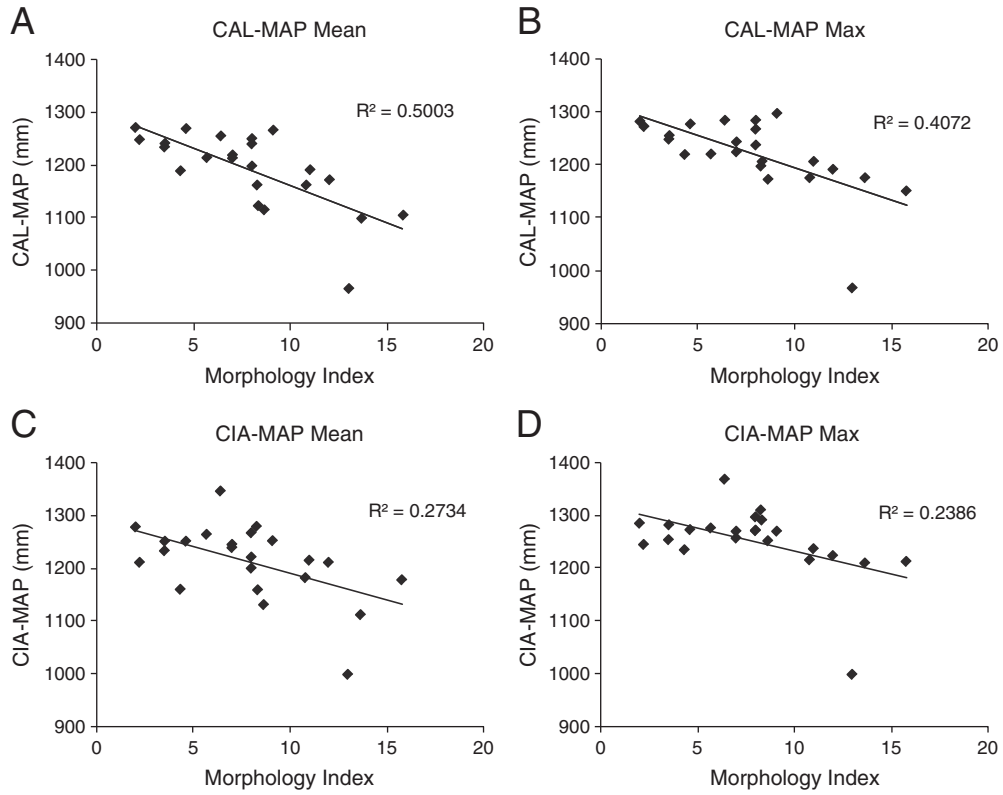


**Fig. 4.** Scatter plots of MAP values versus morphology indices for 23 paleosols in the study area. A. Mean CAL-MAP values calculated for the upper 50 cm of each paleosol plotted against morphology index for each paleosol. B. Maximum CAL-MAP for each paleosol plotted against morphology index. C. Mean CIA-MAP values calculated for the upper 50 cm of each paleosol plotted against morphology index for each paleosol. D. Maximum CIA-MAP for each paleosol plotted against morphology index.

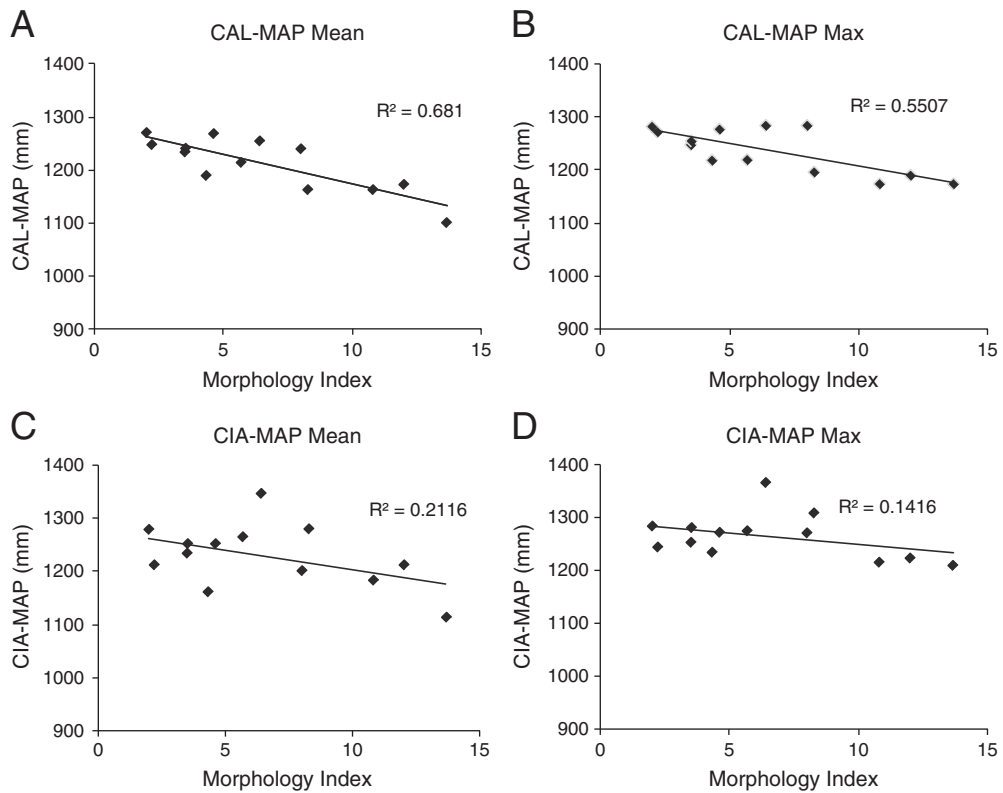


**Fig. 5.** Scatter plots of MAP values versus morphology indices for paleosols with B horizons 1 m thick or thicker. A. Mean CAL-MAP values plotted against morphology index. B. Maximum CAL-MAP value plotted against morphology index. C. Mean CIA-MAP values plotted against morphology index. D. Maximum CIA-MAP values plotted against morphology index.

Regression lines have a negative slope because paleosols with higher morphology indices have features indicating drier soil conditions.

When all 23 paleosols are plotted, the results indicate that increases and decreases in CAL-MAP and CIA-MAP are relatively well correlated to changes in the soil morphology index. The results for CALMAP and morphology index show a much stronger correlation for the mean value of CALMAP (Fig. 4A;  $R^2 = 0.5003$ ) than for the maximum value of CALMAP (Fig. 4B;  $R^2 = 0.4072$ ). The plots of CIA-MAP and morphology index show little difference for the mean and maximum values of MAP ( $R^2 = 0.2734$  and  $0.2386$ ) (Fig. 4C, D); however, in both cases, CIA-MAP shows a weaker correlation to the morphology index than does CALMAP. The results suggest that CALMAP provides a more robust MAP estimate for Vertisols than does CIA-K.

Assessment of the graphs for CAL-MAP and CIA-MAP shows some outliers, usually paleosols that are relatively thin. If paleosols with B horizons thinner than 1 m are eliminated from analysis, a more robust correlation is seen between CAL-MAP and the morphology index (Fig. 5A and B). For the mean CAL-MAP, the  $R^2$  value improves to 0.681 (Fig. 5A). The  $R^2$  value also improves for the maximum value of CAL-MAP ( $R^2 = 0.5507$ ); however, the improvement is less than for the mean value of CAL-MAP. In contrast, the plots for CIA-MAP do not improve if only the thicker paleosols are analyzed (Fig. 5C and D). The Fig. 5 plots include only one paleosol that contains carbonate nodules; the other two carbonate-bearing paleosols were eliminated because both are relatively thin.

## 7. Comparison to other precipitation proxies

The results indicate that increases and decreases in CAL-MAP are relatively well correlated to changes in the soil morphology index. That is one test of the validity of the quantitative method. Yet, the morphology index does not indicate whether the CAL-MAP values for particular paleosols are realistic. Here, we turn to comparison between the quantitative MAP values and paleobotanical estimates of MAP for the study area. The paleobotanical assessment follows other workers who have used paleobotany to evaluate the validity of paleoprecipitation calculated from paleosol weathering indices (e.g., Sheldon et al., 2002; Hamer et al., 2007). The paleosol MAP values all are derived from the Nordt and Driese (2010) method and have the standard error for that technique.

Paleo-MAP estimates have been produced for floras at three stratigraphic levels in the PETM of the southeastern Bighorn Basin (Wing et al., 2005; Peppe et al., 2011). Wing et al. (2005) used leaf size analysis to make MAP estimates for floras near the base and top of the body of the CIE. For each flora, two estimates of MAP were made, one using the modern leaf size/MAP relationship published by Wilf et al. (1998), the other using the leaf size/MAP relationship published by Jacobs and Herendeen (2004), which has more dry sites in the modern data set. The Wilf et al. (1998) regression produced MAP estimates of  $800 + 1140/-560$  mm and  $1440 + 2060/-1000$  mm for the lower and upper floras, respectively (Table 3). The Jacobs and Herendeen (2004) regression

**Table 3**  
Paleobotanical estimates of MAP for paleofloras at three stratigraphic levels in the study areas and CAL-MAP estimates based on paleosols at approximately the same stratigraphic levels. a—Wilf et al. (1998) method; b—Jacobs and Herendeen (2004) method; c—Peppe et al. (2011). Errors for CAL-MAP shown; see text for standard errors of paleobotanical methods.

Stratigraphic interval	Paleosol	CAL-MAP (mm)	Paleobotany (mm)
Upper body of the CIE	HW16-08-05	1189	1320 <sup>a</sup>
	2 paleosols	1271	1440 <sup>b</sup>
Middle body of the CIE	CF07-04	1099	1460 <sup>c,a</sup>
	HW16-08-01	1162	1470 <sup>c</sup>
Lower body of the CIE	HW16-08-19 unit 2	1172	400 <sup>a</sup>
	CF-07-05 unit 4	1248	800 <sup>b</sup>

yielded estimates of 400 mm for the lower flora and 1320 mm for the upper flora. That technique has a standard error of  $\pm 390$  mm. More recently, Peppe et al. (2011) used digital leaf physiognomy to calculate MAP of  $1470 + 1210/-660$  mm for a flora that is near the middle of the body of the CIE, stratigraphically between the floras in Wing et al. (2005). Leaf area analysis produced a nearly identical MAP of  $1460 + 1200/-660$  mm for this flora (Peppe et al., 2011).

Two paleosols at Highway 16 (HW16-08-06 and HW16-08-07), which occur at roughly the same stratigraphic level as the uppermost paleoflora, have calculated MAP values of 1271 mm and 1189 mm (Table 3; Fig. 6). Both values fall below the paleofloral MAP values of 1440 and 1320 mm; however, considering the standard errors for all methods, especially the large standard error for the paleobotanical methods, the results from the paleosol and paleobotanical methods appear relatively consistent. Similarly, a paleosol (CF07-04) that is stratigraphically just below the middle paleoflora has CAL-MAP of 1099 mm. A paleosol at approximately the same stratigraphic level at the Highway 16 location (HW16-08-01) has a similar MAP value of 1162 mm. The paleosol values are less than, but relatively consistent with, the floral MAP estimates (Table 3; Fig. 6).

Finally, two Willwood paleosols are found at approximately the same stratigraphic level as the lowest fossil flora, one at each location (Table 3). The paleosol at Highway 16 (HS16-08-19 unit 2) has calculated MAP of 1172 mm. The roughly time-equivalent paleosol at Cabin Fork (CF-07-05 unit 4) has a MAP of 1248 mm. The paleosol MAP values are relatively consistent with one another and suggest a moderately humid climate; however, the paleosol estimates are much wetter than the paleobotanical estimates of 400 and 800 mm (Fig. 6). These comparisons are troubling because the difference in MAP between the lowermost and uppermost paleofloras ranges from 600 to over 900 mm depending on the technique, yet the MAP estimates for the paleosols at those two stratigraphic levels vary by  $<100$  mm. In particular, the paleosols associated with the lowest paleoflora exceed the plant MAP estimates by as much as 800 mm. All methods have standard errors that provide some latitude when assessing their consistency. Even with a good estimate of leaf area in the original vegetation, there is much scatter in the modern regressions, and

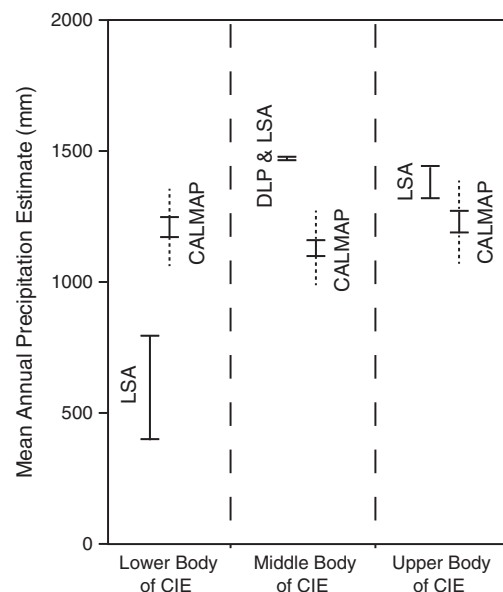


**Fig. 6.** Comparison between paleobotanical estimates of mean annual precipitation and CAL-MAP estimates from paleosols at the same stratigraphic levels. LSA (leaf size analysis) estimates are from Wing et al. (2005) using the Wilf et al. (1998) and Jacobs and Herendeen (2004) approaches; DLP estimate is from Peppe et al. (2011). Dashed lines show standard error for the CALMAP values. See text for standard errors for the paleobotanical methods and Table 3 for MAP estimates.

therefore MAP estimates from leaf size are of very low precision (Wilf et al., 1998). No method has been developed to quantify the effect of the diversity of a floral sample on estimating the true mean leaf size for the vegetation from which the sample was derived; however, samples with few species are bound to vary greatly in how well they represent the mean leaf size of the parent vegetation. The very small number of plant species (6) obtained from the lowest floral site thus provides a poor basis for calculating the average leaf area in the original flora and the MAP under which it grew. We therefore have low confidence in this estimate. The middle and uppermost floras are more diverse, with 29 and 17 species respectively, and for these floras estimates of MAP overlap statistically with those from paleosols.

## 8. Conclusions

Nordt and Driese (2010, p. 410) noted that the bulk soil oxides of Vertisols are largely the product of “calcium carbonate content, inherited clay content, and colloidal based exchangeable cations...”. Consequently, they are distinct from the wide variety of soils on which the CIA-K approach to MAP was developed, and they are better served by a separate approach to MAP. Like the Vertisols on which the CAL-MAG approach was developed, the Willwood paleosols formed on floodplain alluvium with relatively high clay content. The CALMAG technique produces better consistency between MAP estimates and the qualitative assessment of soil moisture determined from morphologic attributes of the Willwood paleosols. Because of this consistency, the CAL-MAP approach appears reliable for detecting up-section changes in soil moisture. That conclusion is reinforced by comparison of the MAP values derived from the Nordt and Driese method to MAP values from paleofloras at the same stratigraphic level as the paleosols. With the exception of the lowest paleoflora, which suffers from small sample size, the MAP values calculated by the two approaches overlap statistically. Because vertic paleosols are common in the stratigraphic record (e.g., Stiles et al., 2001; Driese, 2004; Driese et al., 2005), a paleoprecipitation proxy specifically for this kind of soil will produce more robust paleoclimatic interpretations.

An advantage to the Nordt and Driese (2010) approach is that paleosols with or without carbonate nodules can be analyzed. In paleosol sections formed during times of climatic change, carbonate nodules and carbonate content of the matrix can change significantly. If the paleosols in a stratigraphic section are Vertisols, the CALMAG method allows MAP to be estimated for all of the paleosols. The advantage of the method described by Sheldon et al. (2002) is that it is applicable to a broader array of paleosols.

Thin paleosol profiles (B horizon < 1 m thick) should not be used to determine MAP because the weathering index reflects not only climate, but also the amount of time available for weathering. Thinner paleosols have had less time for weathering and may not have cation distributions representative of precipitation. In addition, the results suggest that better MAP estimates are obtained by taking multiple samples from the upper ~50 cm of the B horizon and averaging the MAP values calculated for each sample.

Finally, this study shows the value of using a soil morphology index for paleoclimatic reconstruction in addition to using a quantitative approach to precipitation. The morphology index provides a simple way to summarize morphologic data that have climatic significance and to compare and contrast different paleosols in a study area. Analyzing multiple proxies produces a more robust climatic interpretation (e.g., Prochnow et al., 2006).

Supplementary materials related to this article can be found online at doi:10.1016/j.palaeo.2011.07.004.

## Acknowledgements

This research was supported by NSF Award EAR0718740 to MJK, NSF Award EAR0717892 to SLW, the Roland W. Brown Fund of the

Smithsonian Institution, and research grants provided by Geological Society of America, Shell Oil/University of Colorado, American Association of Petroleum Geologists, Rocky Mountain Association of Geologists, and the Rocky Mountain Section of Society of Economic Paleontologists and Mineralogists to JSA.

## References

- Becze-Deák, J., Langohr, R., Verrecchia, E.P., 1997. Small scale secondary CaCO<sub>3</sub> accumulations in selected sections of the European loess belt. Morphological forms and potential for paleoenvironmental reconstruction. *Geoderma* 76, 221–252.
- Blodgett, R.H., 1988. Calcareous paleosols in the Triassic Dolores Formation, southwestern Colorado. In: Reinhardt, J., Sigleo, W.R. (Eds.), Geological Society of America Special Paper, 216, pp. 103–121.
- Blodgett, R.H., Crabaugh, J.P., McBride, E.F., 1993. The color of red beds—a geologic perspective. In: Bigham, J.M., Ciolkosz, E.J. (Eds.), Soil Science Society of America Special Publication, 31, pp. 127–159.
- Böhme, M., Ilg, A., Ossig, A., Kuchenhoff, H., 2006. New method to estimate paleoprecipitation using fossil amphibians and reptiles and the middle and late Miocene precipitation gradients in Europe. *Geology* 34, 425–428.
- Bowen, G.J., Bralower, T.J., Delaney, M.L., Dickens, G.R., Kelly, D.C., Koch, P.L., Kump, L.R., Meng, J., Sloan, L.C., Thomas, E., Wing, S.L., Zachos, J.C., 2006. Eocene hyperthermal event offers insight into greenhouse warming. *Eos* 87 (17), 165–169.
- Brady, N.C., Weil, R.R., 1999. The Nature and Properties of Soils, 12th edition. Prentice-Hall, Upper Saddle Ridge, NJ, 881 pp.
- Calero, J., Delgado, R., Delgado, G., Martín-García, J.M., 2008. Transformation of categorical field soil morphological properties into numerical properties for the study of chronosequences. *Geoderma* 145, 278–287.
- Demko, T.M., Currie, B.S., Nicoll, K.A., 2004. Regional paleoclimatic and stratigraphic implications of paleosols and fluvial/overbank architecture in the Morrison Formation (Upper Jurassic), Western Interior, USA. *Sedimentary Geology* 167, 115–135.
- Driese, S.G., 2004. Pedogenic translocation of Fe in modern and ancient Vertisols and implications for interpretations of the Hekpoort paleosol (2.25 Ga). *Journal of Geology* 112, 543–560.
- Driese, S.G., Ober, E.G., 2005. Paleopedologic and paleohydrologic records of precipitation seasonality from Early Pennsylvanian “underclay” paleosols, U.S.A. *Journal of Sedimentary Research* 75, 997–1010.
- Driese, S.G., Nordt, L.C., Lynn, W.C., Stiles, C.A., Mora, C.I., Wilding, L.P., 2005. Distinguishing climate in the soil record using chemical trends in a Vertisol climosequence from the Texas coast prairie, and application to interpreting Paleozoic paleosols in the Appalachian Basin, U.S.A. *Journal of Sedimentary Research* 75, 339–349.
- Evans, C.V., Franzmeier, D.P., 1986. Saturation, aeration, and color patterns in a toposequence of soils in north-central Indiana. *Soil Science Society of America Journal* 50, 975–980.
- Fricke, H.C., Wing, S.L., 2004. Oxygen isotope and paleobotanical estimates of temperature and δ<sup>18</sup>O latitude gradients over North America during the early Eocene. *American Journal of Science* 304, 612–635.
- Fricke, H.C., Clyde, W.C., O’Neil, J.R., Gingerich, P.D., 1998. Evidence for rapid climate change in North America during the latest Paleocene thermal maximum: oxygen isotope compositions of biogenic phosphate from the Bighorn Basin (Wyoming). *Earth and Planetary Science Letters* 160, 193–208.
- Gibson, T.G., Bybell, L.M., Mason, D.B., 2000. Stratigraphic and climatic implications of clay mineral changes around the Paleocene/Eocene boundary of the northeastern US margin. *Sedimentary Geology* 134, 65–92.
- Greenwood, D.R., Wing, S.L., 1995. Eocene continental climates and latitudinal temperature gradients. *Geology* 23, 1044–1048.
- Gregory-Wodzicki, K.M., 2000. Relationships between leaf morphology and climate, Bolivia: implications for estimating paleoclimate from fossil floras. *Paleobiology* 26, 668–688.
- Hamer, J.M.M., Sheldon, N.D., Nichols, G.J., Collinson, M.E., 2007. Late Oligocene–Early Miocene paleosols of distal fluvial systems, Ebro Basin, Spain. *Palaeogeography, Palaeoclimatology, Palaeoecology* 247, 220–235.
- Harden, J.W., 1982. A quantitative index of soil development from field descriptions; examples from a chronosequence in central California. *Geoderma* 28, 1–28.
- Harnois, L., 1988. The CIW index: a new chemical index of weathering. *Sedimentary Geology* 55, 319–322.
- Jacobs, B.F., 1999. Estimation of rainfall variables from leaf characters in tropical Africa. *Palaeogeography, Palaeoclimatology, Palaeoecology* 145, 231–250.
- Jacobs, B.F., Herendeen, P.S., 2004. Eocene dry climate and woodland vegetation in tropical Africa reconstructed from fossil leaves from northern Tanzania. *Palaeogeography, Palaeoclimatology, Palaeoecology* 213, 115–123.
- Kraus, M.J., Hasiotis, S.T., 2006. Significance of different modes of rhizolith preservation to interpreting paleoenvironmental and paleohydrologic settings: examples from Paleogene paleosols, Bighorn Basin, Wyoming, U.S.A. *Journal of Sedimentary Research* 76, 633–646.
- Kraus, M.J., Riggins, S., 2007. Transient drying during the Paleocene–Eocene Thermal Maximum (PETM): analysis of paleosols in the Bighorn Basin, Wyoming. *Palaeogeography, Palaeoclimatology, Palaeoecology* 245, 444–461.
- Lynn, W.C., Williams, D., 1992. The making of a Vertisol. *Soil Survey Horizons* 33, 45–50.
- Marbut, C.F., 1935. Atlas of American Agriculture. III. Soils of the United States. Government Printing Office, Washington, D.C. 98 pp.
- Maynard, J.B., 1992. Chemistry of modern soils as a guide to interpreting Precambrian paleosols. *Journal of Geology* 100, 279–289.

- McKenzie, R.M., 1989. Manganese oxides and hydroxides. In: Dixon, J.B., Weed, S.B. (Eds.), *Minerals in Soil Environments*, Second edition. Soil Science Society of America, pp. 439–465.
- Nordt, L.C., Driese, S.G., 2010. New weathering index improves paleorainfall estimates from Vertisols. *Geology* 38, 407–410.
- Nordt, L.C., Orosz, M., Driese, S.G., Tubbs, J., 2006. Vertisol carbonate properties in relation to mean annual precipitation: implications for paleoprecipitation estimates. *Journal of Geology* 114, 501–510.
- Peppe, D.J., Royer, D.L., Cariglino, B., Oliver, S.Y., Newman, S., Leight, E., Enikolopov, G., Fernandez-Burgos, M., Herrera, F., Adams, J.M., Correa, E., Currano, E.D., Erickson, J.M., Hinojosa, L.F., Iglesias, A., Jaramillo, C.A., Johnson, K.R., Jordan, G.J., Kraft, N., Lovelock, E.C., Lusk, C.H., Niinemets, Ü., Peñuelas, J., Rapson, G., Wing, S.L., Wright, I.J., 2011. Sensitivity of leaf size and shape to climate: global patterns and paleoclimatic applications. *The New Phytologist* 190, 724–739.
- PiPujol, M.D., Buurman, P., 1994. The distinction between ground-water gley and surface-water gley phenomena in Tertiary paleosols of the Ebro Basin, NE Spain. *Palaeogeography, Palaeoclimatology, Palaeoecology* 10, 103–113.
- PiPujol, M.D., Buurman, P., 1997. Dynamics of iron and calcium carbonate redistribution and palaeohydrology in middle Eocene alluvial paleosols of the southeast Ebro Basin margin (Catalonia, northeast Spain). *Palaeogeography, Palaeoclimatology, Palaeoecology* 134, 87–107.
- Prochnow, S.J., Nordt, L.C., Atchley, S.C., Hudec, M.R., 2006. Multi-proxy paleosol evidence for middle and late Triassic climate trends in eastern Utah. *Palaeogeography, Palaeoclimatology, Palaeoecology* 232, 53–72.
- Ransom, M.D., Smeck, N.E., Bigham, J.M., 1987. Micromorphology of seasonally wet soils on the Illinoian till plain, USA. *Geoderma* 40, 83–99.
- Retallack, G.J., 1991. Untangling the effects of burial alteration and ancient soil formation. *Annual Review of Earth and Planetary Science* 19, 183–206.
- Retallack, G.J., 1994. The environmental factor approach to the interpretation of paleosols. In: Amundson, R., Hardin, J., Singer, M. (Eds.), *Soil Science Society of America Special Publication*, 33, pp. 31–64.
- Royer, D.L., 1999. Depth to pedogenic carbonate horizon as a paleoprecipitation indicator. *Geology* 27, 1123–1126.
- Schwertmann, U., Fanning, D.S., 1976. Iron–manganese concretions in hydrosequences of soils in loess in Bavaria. *Soil Science Society of America Journal* 40, 731–738.
- Sheldon, N.D., Tabor, N.J., 2009. Quantitative paleoenvironmental and paleoclimatic reconstruction using paleosols. *Earth-Science Reviews* 95, 1–52.
- Sheldon, N.D., Retallack, G.J., Tanaka, S., 2002. Geochemical climofunctions from North American soils and application to paleosols across the Eocene–Oligocene boundary in Oregon. *Journal of Geology* 110, 687–696.
- Smith, F.A., Wing, S.L., Freeman, K.H., 2007. Magnitude of the carbon isotope excursion at the Paleocene–Eocene thermal maximum. The role of plant community change. *Earth and Planetary Science Letters* 262, 50–65.
- Smith, J.J., Hasiotis, S.T., Kraus, M.J., Woody, D.T., 2008. Relationship of floodplain ichnocoenoses to paleopedology, paleohydrology, and paleoclimate in the Willwood Formation, Wyoming, during the Paleocene–Eocene Thermal Maximum. *Palaios* 23, 683–699.
- Soil Survey Division Staff, 1993. *Soil survey manual*. Soil Conservation Service. U.S. Department of Agriculture Handbook, 18. 532 pp.
- Stiles, C.A., Mora, C.I., Driese, S.G., 2001. Pedogenic iron–manganese nodules in Vertisols: a new proxy from paleoprecipitation? *Geology* 29, 943–946.
- van Dam, J.A., 2006. Geographic and temporal patterns in the late Neogene (12–3 Ma) aridification of Europe: the use of small mammals as paleoprecipitation proxies. *Palaeogeography, Palaeoclimatology, Palaeoecology* 238, 190–218.
- Veneman, P.L.M., Spokas, L.A., Lindbo, D.L., 1998. Soil moisture and redoximorphic features: a historical perspective. In: Rabenhorst, M.C., Bell, J.C., McDaniel, P.A. (Eds.), *Soil Science Society of America Special Publication*, 54, pp. 1–23.
- Vepraskas, M.J., 2001. Morphological features of seasonally reduced soils. In: Richardson, J.J., Vepraskas, M.J. (Eds.), *Wetland Soils: Genesis, Hydrology, Landscapes, and Classification*. Lewis Publishers, Boca Raton, FL, pp. 163–182.
- Vidic, N.J., Lobnik, F., 1997. Rates of soil development of the chronosequence in the Ljubljana Basin, Slovenia. *Geoderma* 76, 35–64.
- Wells, N.A., Konowal, M., Sundback, S.A., 2002. Quantitative evaluation of color measurements II. Analysis of Munsell color values from the Colton and Green River Formations (Eocene, central Utah). *Sedimentary Geology* 151, 17–44.
- White, G.N., Dixon, J.B., 1996. Iron and manganese distribution in nodules from a young Texas Vertisol. *Soil Science Society of America Journal* 60, 1254–1262.
- Wiemann, M.C., Manchester, S.R., Dilcher, D.L., Hinojosa, L.F., Wheeler, E.A., 1998. Estimation of temperature and precipitation from morphological characters of dicotyledonous leaves. *American Journal of Botany* 85, 1796–1802.
- Wilf, P., Wing, S.L., Greenwood, D.R., Greenwood, C.L., 1998. Using fossil leaves as paleoprecipitation indicators: an Eocene example. *Geology* 26, 203–206.
- Wing, S.L., Harrington, G.J., Smith, F.A., Bloch, J.I., Boyer, D.M., Freeman, K.H., 2005. Transient floral change and rapid global warming at the Paleocene–Eocene boundary. *Science* 310, 993–996.
- Wolfe, J.A., 1995. Paleoclimatic estimates from Tertiary leaf assemblages. *Annual Reviews of Earth and Planetary Sciences* 23, 119–142.
- Wolfe, J.A., Spicer, R.A., 1999. Fossil leaf character states: multivariate analyses. In: Jones, T.P., Rowe, N.P. (Eds.), *Fossil Plants and Spores: Modern Techniques*. Geological Society of London, London, pp. 233–239.